Impact of the Low Wavenumber Structure in the Initial Vortex Wind Analyses on the Prediction of the Intensification of Hurricane Patricia (2015)

Key Points:

- Spin-up (SPU) members showed more significant azimuthal asymmetry than spin-down (SPD) members in the initial wind analyses
- Low wavenumber components dominated the differences between the SPD and SPU members
- The low wavenumber structure of the initial wind analyses was important in predicting the intensity changes of Hurricane Patricia (2015)

Correspondence to:

X. Wang and R. Ding,
xuguang.wang@ou.edu;
drq@bnu.edu.cn

Author Contributions:

Conceptualization: Quanjia Zhong, Xuguang Wang, Ruiqiang Ding
Funding acquisition: Quanjia Zhong, Xuguang Wang, Ruiqiang Ding
Investigation: Quanjia Zhong
Supervision: Xuguang Wang, Ruiqiang Ding
Writing – original draft: Quanjia Zhong
Writing – review & editing: Quanjia Zhong, Xuguang Wang, Ruiqiang Ding, Xu Lu, Yongjie Huang, Wansuo Duan, Lei Liu

Quanjia Zhong[1,2] [ID]**, Xuguang Wang[2]** [ID]**, Ruiqiang Ding[1,3]** [ID]**, Xu Lu[2]** [ID]**, Yongjie Huang[2]** [ID]**, Wansuo Duan[1]** [ID]**, and Lei Liu[4]** [ID]

[1]State Key Laboratory of Numerical Modeling for Atmospheric Sciences and Geophysical Fluid Dynamics (LASG), Institute of Atmospheric Physics, Chinese Academy of Sciences, Beijing, China, [2]School of Meteorology, University of Oklahoma, Norman, OK, USA, [3]State Key Laboratory of Earth Surface Processes and Resource Ecology, Beijing Normal University, Beijing, China, [4]College of Meteorology and Oceanology, National University of Defense Technology, Changsha, China

Abstract Ensemble clustering analysis was performed to explore the role of the initial hurricane vortex-scale wind structure in the prediction of the intensification of Hurricane Patricia (2015). Convection-allowing ensemble forecasts were classified into spin-down (SPD) and spin-up (SPU) groups. Specifically, 10 members with an intensification rate >0 m/s and 10 members with an intensification rate <0 m/s for the first 6 hr were defined as the SPD and SPU members. The result showed that the tangential winds outside the inner-core region in the SPD members were weaker compared to the SPU members. Additionally, the SPD members had a weaker inflow near the surface and a weaker outflow between the heights of 8 and 12 km than the SPU members. The SPU members showed more significant azimuthal asymmetry than the SPD members in the surface, tangential and radial winds. Wavenumber analysis showed that the low wavenumber components dominated the differences between the SPD and SPU members. Numerical experiments were conducted to test the hypothesis generated by the clustering analysis. It was found that the storm's maximum wind speed (MWS) intensified during the first 6 hr of the model forecast if only the low wavenumber structure in the SPU members was included in the initial conditions, whereas it decayed during the first 6 hr if only the low wavenumber structure in the SPD members was included. This result confirms that the low wavenumber structure of the initial wind analyses was important in predicting the intensity changes of Hurricane Patricia (2015).

Plain Language Summary Accurate forecasts of the intensity of tropical cyclones (TCs) are important in both early warning systems and impact assessments. However, the spin-down (SPD) issue remains a challenge in the operational HWRF model and occurs in many TC cases, especially in the prediction of intense TCs, which can lead to substantial degradation of the short-term intensity forecast. In this paper, ensemble clustering analysis was performed to explore the role of the initial hurricane vortex-scale wind structure in the prediction of the intensification of Hurricane Patricia (2015). Convection-allowing ensemble forecasts were classified into spin-down (SPD) and spin-up (SPU) groups. Several statistically significant differences were found in the structure of the initial vortex wind analyses between the SPD and SPU members. Particularly, the low wavenumber components dominated the differences between the SPD and SPU members. Both the wavenumber analysis and numerical experiments suggested that the low wavenumber structure of the initial wind analyses in ensemble members was important in predicting the intensity changes of Hurricane Patricia (2015). These results would be helpful as a way for alleviating the SPD issue in the operational HWRF model system.

1. Introduction

Accurate forecasts of the intensity of tropical cyclones (TCs) are important in both early warning systems and impact assessments because the damage caused by these storms is significantly associated with their intensity. Previous studies have suggested that changes in the intensity of TCs are affected by the dynamic and thermodynamic structures of the inner core, multiscale interactions between the storm and the environmental flow, and the asymmetry of the storm (Brown & Hakim, 2015; Chen et al., 2019; Rogers et al., 2013; Vukicevic et al., 2014). It remains a challenge to improve operational forecasts of the change in intensity of TCs, especially during the rapid

intensification stage, despite recent developments in numerical models, substantial increases in the number of observations of the inner core region, and the use of advanced data assimilation methods (Cangialosi et al., 2020; DeMaria et al., 2014; Emanuel & Zhang, 2016).

Hurricane Patricia (2015) was a category-5 hurricane on the Saffir–Simpson wind scale. It formed in the eastern Pacific at about 0600 UTC 20 October 2015 and made landfall near Cuixmala on the southwestern coast of Mexico on 23 October 2015. Rogers et al. (2017) reported that it was the strongest TC ever recorded in terms of wind speed, with a maximum sustained wind of 95.2 m/s (185 knots). The intensity also changed at an unprecedented rate (54 m/s in 24 hr), much greater than the rapid intensification threshold [15.4 m/s in a 24-hr period, Kaplan & DeMaria, 2003]. Unfortunately, most of the operational dynamical and statistical–dynamical models were unable to predict the rapid intensification and peak intensity of this storm. All the main operational models, such as the Geophysical Fluid Dynamics Laboratory and Hurricane Weather Research and Forecasting (HWRF) models, predicted a peak intensity below category 2 (Qin & Zhang, 2018).

It has been reported that the forecast skill for the intensity of Hurricane Patricia (2015) could be improved by increasing the spatial resolution of the model, assimilating novel observations, and modifying the model physics (e.g., the microphysics and planetary boundary layer schemes) in retrospective forecasts (Feng and Wang, 2019, 2021; Lu & Wang, 2019; Nystrom & Zhang, 2019; Qin & Zhang, 2018). For instance, as a result of the small size of Hurricane Patricia (2015), which had a radius of maximum wind (RMW) of about 18 km, higher model resolutions have been shown to better resolve the storm structure and therefore significantly improve the prediction skill during the rapid intensification period (Feng & Wang, 2019; Qin & Zhang, 2018). Lu and Wang (2019) found that a major source of errors in the intensity forecasts was a model spin-down (SPD) issue (as depicted by the maximum decrease in the sustained wind speed) during the initial stages of rapid intensification, even though the analyzed vortex was initialized with a more realistic analysis produced by an advanced data assimilation system. They subsequently found that modifying the turbulent mixing parameterization and reducing the horizontal diffusion could potentially alleviate the model SPD issue.

Moreover, the SPD issue remains a challenge in the operational HWRF model and occurs in many TC cases, especially in the prediction of intense TCs, which can lead to substantial degradation of the short-term intensity forecast (Tong et al., 2018). Considering the fact that Hurricane Patricia (2015) was the most intense TC on record in the eastern North Pacific, we used the analysis ensemble generated by Lu and Wang (2019) to explore the impact of the initial conditions on the rapid intensification of Hurricane Patricia. Although the control member of the ensemble of Lu and Wang (2019) captured the spin-up (SPU) process of the storm during the initial stages of rapid intensification, persistent SPD remained in the forecasts of some ensemble members (Figure 1). Given that these ensemble forecasts only differ in their initial conditions, this dataset provides a route toward understanding the impact of the initial conditions on the development and maintenance of the vortex. Past studies have suggested that the quality of the initial conditions is crucial in the numerical prediction of rapid changes in the hurricane track, intensity and structure (Lang et al., 2012; Leutbecher & Palmer, 2008; Toth & Kalnay, 1997; Wang et al., 2020). It is also well known that there is a decrease in the surface fluxes of latent heat when cold sea surface temperatures or land are encountered, leading to SPD of the hurricane vortex (Reasor et al., 2000).

None of these studies, however, focused on the role of the different scales of structures in the initial TC wind analyses in determining changes in the intensity of the hurricanes. In early studies, the structural asymmetry of the TC wind speed and vortices was hypothesized to affect the intensification of the storm (Montgomery et al., 2001; Tong et al., 2018; Zhou et al., 2015). Through diagnosing the differences in the initial TC wind analyses between the SPD and SPU groups, so-called ensemble clustering analysis, we address the following scientific questions in this paper: (a) What are the statistically significant differences in the initial TC wind fields between the SPD and SPU members? (b) Which wave numbers of the initial vortex wind analyses of a TC dominate such differences?

The rest of this paper is arranged as follows. Section 2 presents the model configuration, experimental setup, and methods. Section 3 investigates the differences in the initial analyses and forecasts between the ensemble members with SPD and SPU processes. Concluding remarks and further discussion are given in Section 4.
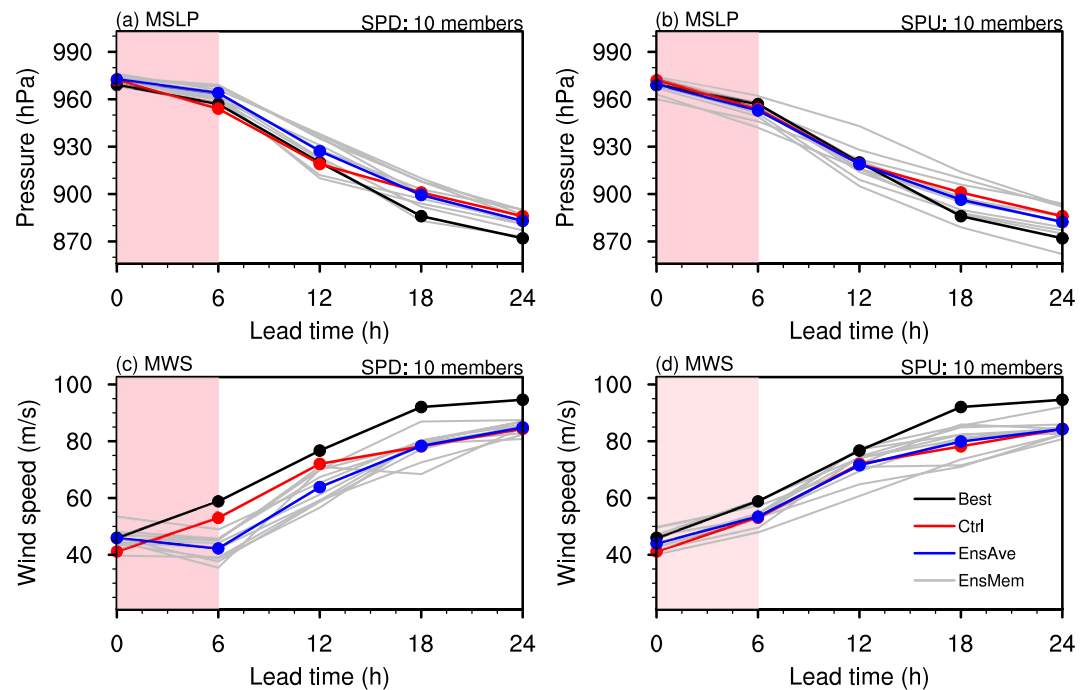
Figure 1. Forecasts of the minimum sea-level pressure (MSLP; unit: hPa) and maximum wind speed (MWS; unit: m/s) as a function of lead time for the (a), (c) spin-down (SPD) and (b), (d) spin-up (SPU) members. The gray lines represent the ensemble members (EnsMem) and the blue line represents the ensemble average (EnsAve). The red and black lines represent the control (Ctrl) and best-track (Best) forecasts. The light pink shading shows the lead time over the first 6 hr of the model forecast.

2. Data and Methods

2.1. Model Configuration and Experiment Setup

The ensemble of analyses adopted was produced by a gridpoint statistical interpolation (GSI)-based, continuously cycled, dual-resolution hybrid ensemble–variational (EnVar) data assimilation system developed by Lu and Wang (2019). The model was triple-nested with horizontal resolutions of 18/6/2 km (0.1358°/0.0458°/0.0158°), following the 2015 operational HWRF model configuration. The model has 61 vertical levels with the top of the model at 2 hPa. The basic model physics included the Ferrier–Aligo microphysics scheme (Schoenberg Ferrier, 1994), the simplified Arakawa–Schubert cumulus scheme (Han & Pan, 2006), the HWRF modified surface layer scheme (Kwon et al., 2010), the HWRF planetary boundary layer scheme (Hong & Pan, 1996), and the Rapid Radiative Transfer Model for General Circulation Models longwave and shortwave radiation schemes (Lacis & Hansen, 1974; Schwarzkopf & Fels, 1991). The analysis ensemble was created by assimilating routine observational data and was composed of 1 control member and 40 ensemble members with recentered analyses.

To better resolve the small size of Hurricane Patricia (2015), the HWRF model was triple-nested during the ensemble forecast with horizontal resolutions of 9/3/1 km for the outermost (288×576 grid points), intermediate (304×604 grid points) and innermost (303×601 grid points) domains, respectively. The initial conditions were therefore interpolated to a higher horizontal resolution of 9/3/1 km.

The boundary conditions for the outermost domain were provided by the National Centers for Environmental Prediction Global Forecasting System. We carried out one set of retrospective HWRF ensemble forecasts of Hurricane Patricia (2015) at 1200 UTC 22 October 2015 for the early stages of rapid intensification, and the experiments were output for 24 hr at 6-hr output intervals. The best-track estimates for Hurricane Patricia (2015) were obtained from the National Hurricane Center.

Table 1
Rate of Change in Maximum Wind Speed During the First 6 hr of the Model Forecast for the Spin-Down (SPD) and Spin-Up (SPU) Members

	SPD		SPU	
	Member	Increment (m/s)	Member	Increment (m/s)
1	Ens02	−8.23	Ens06	6
2	Ens03	−0.51	Ens07	10.29
3	Ens09	−9.26	Ens08	10.81
4	Ens22	−1.03	Ens13	7.72
5	Ens24	−0.51	Ens14	10.29
6	Ens25	−2.57	Ens17	11.83
7	Ens32	−2.06	Ens20	11.83
8	Ens36	−5.14	Ens28	10.80
9	Ens38	−4.63	Ens35	7.20
10	Ens40	−2.05	Ens37	7.72
			Ctrl	
	Mean	−3.61	Mean	9.46

2.2. Wavenumber Decomposition

We used wavenumber decomposition, the mathematical representation for the Fourier transform, to obtain the spectral components of a given 2D variable field (Vukicevic et al., 2014):

$$\widehat{V}(k) = \int_{-\infty}^{\infty} V(x)e^{-2\pi ixk}dx, \tag{1}$$

where $V(x)$ is the spatial representation (e.g., a 2D gridded field) for the variable and $\widehat{V}(k)$ is the respective frequency (e.g., wave number) spectrum resulting from the Fourier transform. The 2D field was projected as a function of the radial distance at 5-km intervals and the azimuth at 5° intervals relative to the storm center, and then computed using the discrete fast Fourier transform. It was found that the results of the wavenumber analysis were not sensitive to the choice of interval for the radial distance and azimuth. Then, we evaluated the structural asymmetry of the hurricane in the inner core region using model-derived wind data within 150 km from the storm center. A two-tailed Student's *t*-test was performed on selected aspects of the wind speed fields to determine whether the ensemble-mean values of the storm structure differed significantly from each other at 95% confidence levels.

3. Results

3.1. Differences Between the SPD and SPU Members in the Analyses and Forecasts

Figure 1 shows the forecasts of the minimum sea-level pressure (MSLP) and maximum wind speed (MWS) along with the best-track estimates (black line) from the National Hurricane Center. Consistent with previous studies, there was SPD in the deterministic forecast, but persistent SPD remained in the forecasts of some ensemble members. This suggests that the forecast skill for the TC intensity at shorter lead times is highly dependent on the initial conditions because the ensemble and control members only differed in their initial analysis. We therefore analyzed the differences in the initial conditions between the SPD and SPU members.

From the 40 ensemble members, based on the rate of change in MWS intensity at the first 6 hr, 10 members with an intensification rate <0 m/s and 30 members with an intensification rate >0 m/s (a decrease in wind speed for the first 6 hr) were defined as the SPD and the SPU members, respectively. Among the ensemble members, 75% and 25% were SPU and SPD members, respectively, and the total number of SPD members was less than that of the SPU members. To make the total number match in each group, we randomly selected 10 SPU members and 10 SPD members, which were classified into the SPD and SPU groups. Considering the fact that the control member could capture the SPU process of the storm during the initial stages of rapid intensification, it could be regarded as one of the SPU members and so we do not discuss it separately any further in this paper. The negative and positive values for the rate of change in MWS during the first 6 hr (Figures 1c and 1d) are summarized in Table 1. The average rate of change in MWS was −3.61 m/s for the SPD members and 9.46 m/s for the SPU members. The most significant weakening of the SPU members during the first 6 hr was seen for ensemble member (Ens) 09, with a rate of change in intensity of −9.26 m/s, whereas the most significant increase in intensity for the SPU members was 11.83 m/s, for Ens 17 and 20. Different from MWS, a 24-hr decrease in MSLP was present in both the SPD and SPU members, and the average MSLP reached about 885 hPa at a lead time of 24 hr (Figures 1a and 1b). As pointed out by Lu and Wang (2019), the difference in evolution between MWS and MSLP was probably associated with the deficiency in the HWRF model's physics insofar as it being unable to maintain realistic storm structures from the initial analysis.

Moreover, the ensemble spread of the MSLP in the first 6 hr for the SPD group was smaller than that for the SPU group, but the ensemble spread of the MWS in the SPD group was larger than that for the SPU group in the same period (not shown). This result indicates that, in the initial few hours, the SPD group had relatively low uncertainty in its MSLP but relatively high uncertainty in its MWS, as compared with the SPU group.
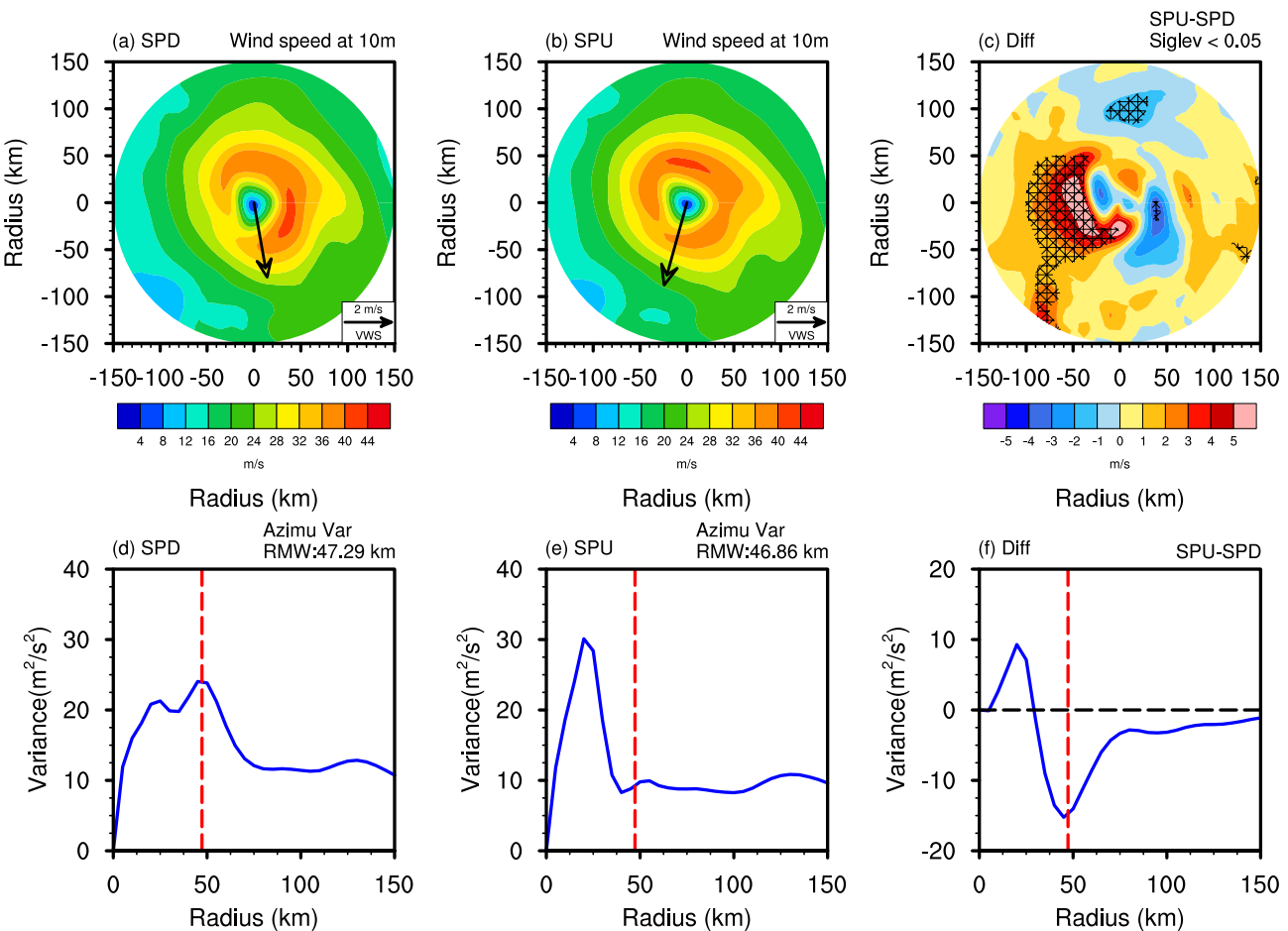
Figure 2. Average of the azimuthal surface wind speed (shading; unit: m/s) and the mean azimuthally averaged variances of the surface wind speed for the (a), (d) SPD and (b), (e) SPU members at the initial time. (c), (f) Differences in the azimuthal wind speed and azimuthally averaged variances between the SPD and SPU members (SPU − SPD). The red dashed line is the average radius of maximum wind (RMW) at the height of 10 m. The black dashed line is the reference zero line. The gridded regions indicate statistical significance at the 95% confidence level. The black arrow is the vertical wind shear (VWS) vector. Note that the surface wind field indicates the wind field at the height of 10 m.

We calculated the average azimuthal wind speed structure at 10 m within 150 km of the center of the storm and its azimuthal variance as a function of the radial distance to determine the differences in the initial storm structure between the SPD and SPU members (Figure 2). Although the magnitude of the maximum surface wind speed for the SPD members was comparable with that of the SPU members, they showed significant differences in the location of the MWS. The ensemble mean of the wind speed field at 1200 UTC 22 October 2015 for the SPD members represented a relatively large storm (RMW of ∼47.29 km) with the maximum surface wind speed (∼40 m/s) to the southeast (Figure 2a), whereas that of the SPU members represented a slightly smaller storm (RMW of ∼46.86 km) with the maximum surface wind speed (∼40 m/s) to the north (Figure 2b). The wind speed in the west of the storm was weaker for the SPD members than for the SPU members (significant at the 95% confidence level), but their differences in the southeast of the storm were not significant at the 95% confidence level (Figure 2c).

The relatively large size of the storm structure for the SPD members was also seen in the azimuthal variances of the surface wind speed. The azimuthal variance as a function of the radial distance represents the asymmetrical structure of the storm in the surface layer. There is a large asymmetric variance inside the RMW in SPU members while the asymmetric variance is large near the RMW (nearly in the eyewall of a TC vortex) in the SPD members (Figures 2d and 2e). As shown in Figure 2f, the asymmetry inside the radius of ∼25 km was weaker for the SPD members than for the SPU members, but the opposite was true outside the radius of ∼25 km. This result suggests that the asymmetric structure in the eyewall is key to the SPU of the model TC. Such systematic differences of
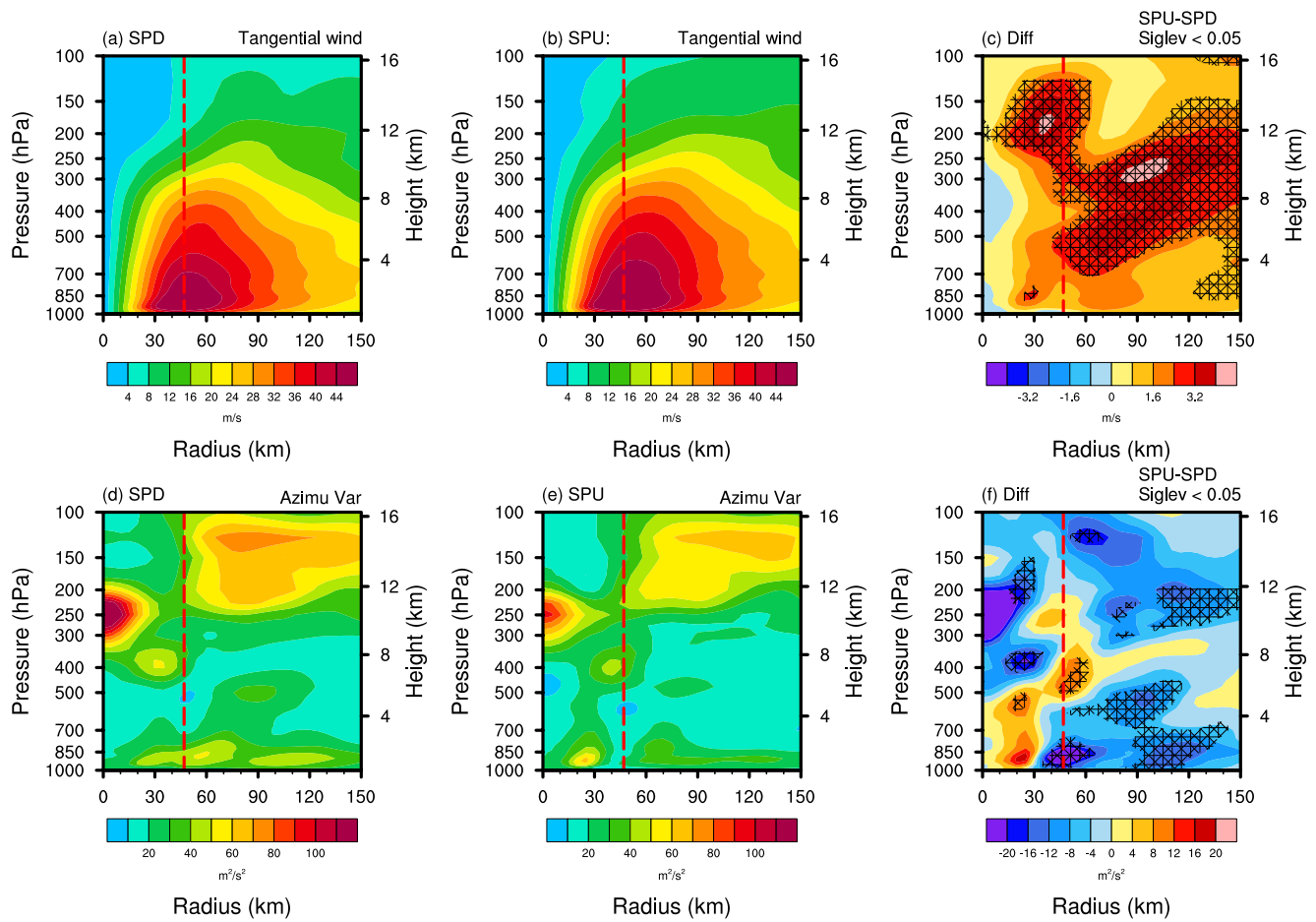
Figure 3. Radius–height plots of the ensemble-average azimuthal mean tangential wind speed (unit: m/s) and the variance of tangential wind (unit: m²/s²) for the (a), (d) SPD and (b), (e) SPU members. (c), (f) Differences in the azimuthal mean tangential wind speed (unit: m/s) and the azimuthal variance of tangential wind speed between the SPD and SPU members (SPU − SPD). The red dashed line is the average RMW at the height of 10 m. The gridded regions indicate statistical significance at the 95% confidence level.

the asymmetry of the SPU members relative to the SPD members are consistent with earlier modeling studies and observations of Patricia (2015). Based on airborne doppler observations, Rogers et al. (2013) reported that intensifying storms have a ring-like asymmetrical structure inside the RMW. More recently, Montgomery et al. (2020), using idealized simulations of TCs, showed that wind asymmetries, associated in part with asymmetrical deep convection, make an important contribution to the MWS inside the RMW. A sequence of infrared satellite imagery showed that Hurricane Patricia (2015) had asymmetrical convection in the inner core early in its development during a 6-hr period when the MWS increased by 28.3 m/s (Callaghan, 2017).

Figures 3a and 3b compare the ensemble-average azimuthal mean tangential wind speed for the SPD and SPU members. The tangential wind structures for both the SPD and SPU members also exhibited a single (primary) eyewall with velocity maximized around the RMW and rapidly decreasing vertically as well as radially outward from the RMW. This suggests that the difference in the axisymmetric structure might not be the key factor triggering the difference in the SPD and SPU ensembles since Rogers et al. (2013) showed that such structure is often observed in intensifying TCs. As can be seen from Figure 3c, the structure of the primary circulation inside the RMW below the height of 10 km showed very little difference between the SPD and SPU members. The azimuthal mean tangential wind speed >60 km from the center of the storm between the heights of 4 and 12 km was significantly larger for the SPU members than for the SPD members (significant at the 95% confidence level), probably because the latter had a stronger decaying wind field than the former between those heights.

It is known that an asymmetric structure can be associated with environmental forcing (Chen & Gopalakrishnan, 2015; Jones, 1995; Wang & Holland, 1996). Therefore, we further examined the relationship

between the asymmetric structure and the deep-layer vertical wind shear. Given the small size of Hurricane Patricia, the local vertical shear was calculated using the difference between the horizontal winds at the 850- and 200-hPa levels, averaged within a 150-km-radius circle centered on the TC center. As shown in Figures 3a and 3b, there was little difference in the magnitude of vertical shear between the SPD and SPU members (4.05 m/s vs. 4.13 m/s), while their asymmetric winds had an almost opposite phase relationship with the vertical wind shear. When the initial asymmetry was in phase with the asymmetry forced by the vertical shear (e.g., downshear-left), the asymmetry would be enhanced and could cause the SPD issue. In contrast, in the SPU members, the initial surface wind in the inner core region exhibited a pronounced asymmetry whose maxima were located in the upshear-right quadrant. Such an anti-phased relationship between the direction of deep-layer vertical wind shear and eyewall convection may have partially offset the asymmetry and favored the storm's intensification. This result is consistent with the study of Reasor et al. (2009), who suggested that initially upshear-right convective cells will intensify and coalesce into mesoscale clusters during their rotation through the downshear eyewall. Although this argument is physically reasonable, the hypothesis itself is worthy of a future study to verify.

Figures 3d and 3e compare the ensemble-average azimuthal variance of the tangential wind speed for the SPD and SPU members using radius–height plots. Such plots are used to show the asymmetrical characteristics of the 3D storm structures. Although the maximum azimuthal variance in the upper level of the storm center was greater for the SPD members than for the SPU members, the difference was not significant at the 95% confidence level. As shown in Figures 3f and 3a significant difference in the maximum azimuthal variance between the SPU and SPD members occurred in the inner core, about 25 km from the center of the storm below the height of 6 km. At mid and low levels between 0 and 8 km, there were positive values of variance difference inside the RMW and negative values outside (Figure 3f). These results suggest that the variance of the SPU members inside the RMW was larger than that of the SPD members, while the former was smaller than the latter outside the RMW.

The distinction between the SPU and SPD members remained negative outside the RMW up to an outermost radius of 150 km (significant at the 95% confidence level). This result is consistent with Figure 2f, which shows that the asymmetry of the storm in the outer core region was stronger for the SPD members than for the SPU members (Figure 3f). However, there was less distinction above 12 km than at mid and lower levels. Previous observational studies have also suggested that such asymmetrical structure can be found in other TC variables (Callaghan, 2017; Persing et al., 2013; Reasor et al., 2009; Rogers et al., 2013). For example, intensifying TCs have a ring-like asymmetrical structure of vertical vorticity and reflectivity inside the RMW (Rogers et al., 2013). The period of anomalous intensification is modulated by internally generated vorticity asymmetries (Reasor et al., 2009). Moreover, asymmetrical inner-core convection, especially in the early stages of rapid intensification, leads to storm intensification (Persing et al., 2013).

Figures 4a and 4b compare the ensemble-average azimuthal mean radial wind speed for the SPD and SPU members. Both sets of members shared several structural similarities in their radial wind: the maximum radial inflow in the lowest 1-km height layer; an area of outflow at a height of approximately 12 km; and a peak in outflow at the upper level. Although the outflow at the upper level was stronger for the SPD members than for the SPU members, the difference was not significant at the 95% confidence level. There were two statistically significant differences in the structure of the radial flow between the SPD and SPU members. The storm structure for the SPD members had a weaker inflow near the surface compared with the SPU members, as well as a weaker outflow between the heights of 8 and 12 km, both significant at the 95% confidence level (Figure 4c). As highlighted by Montgomery and Smith (2018) and Smith et al. (2009), a stronger inflow in the lowest 1-km height layer favors a larger SPU of the tangential winds in the boundary layer and therefore rapid intensification.

Figures 4d and 4e show the ensemble-average azimuthal variance of the radial wind for the SPD and SPU members. There was a similar structure of the azimuthal variance for the SPD and SPU members, but the magnitude of the peak azimuthal variance for the SPD members was greater than that of the SPU members at both lower and upper levels (significant at the 95% confidence level), suggesting that persistent SPD processes were associated with the asymmetry of the lower inflow and upper outflow (Figure 4f).

3.2. Wavenumber Analysis of the Initial Wind Fields

Many studies have found that the structure and evolution of rapidly intensifying hurricanes may be related to the low azimuthal wavenumber component of the vortex (Reasor et al., 2000, 2009). We therefore applied Fourier
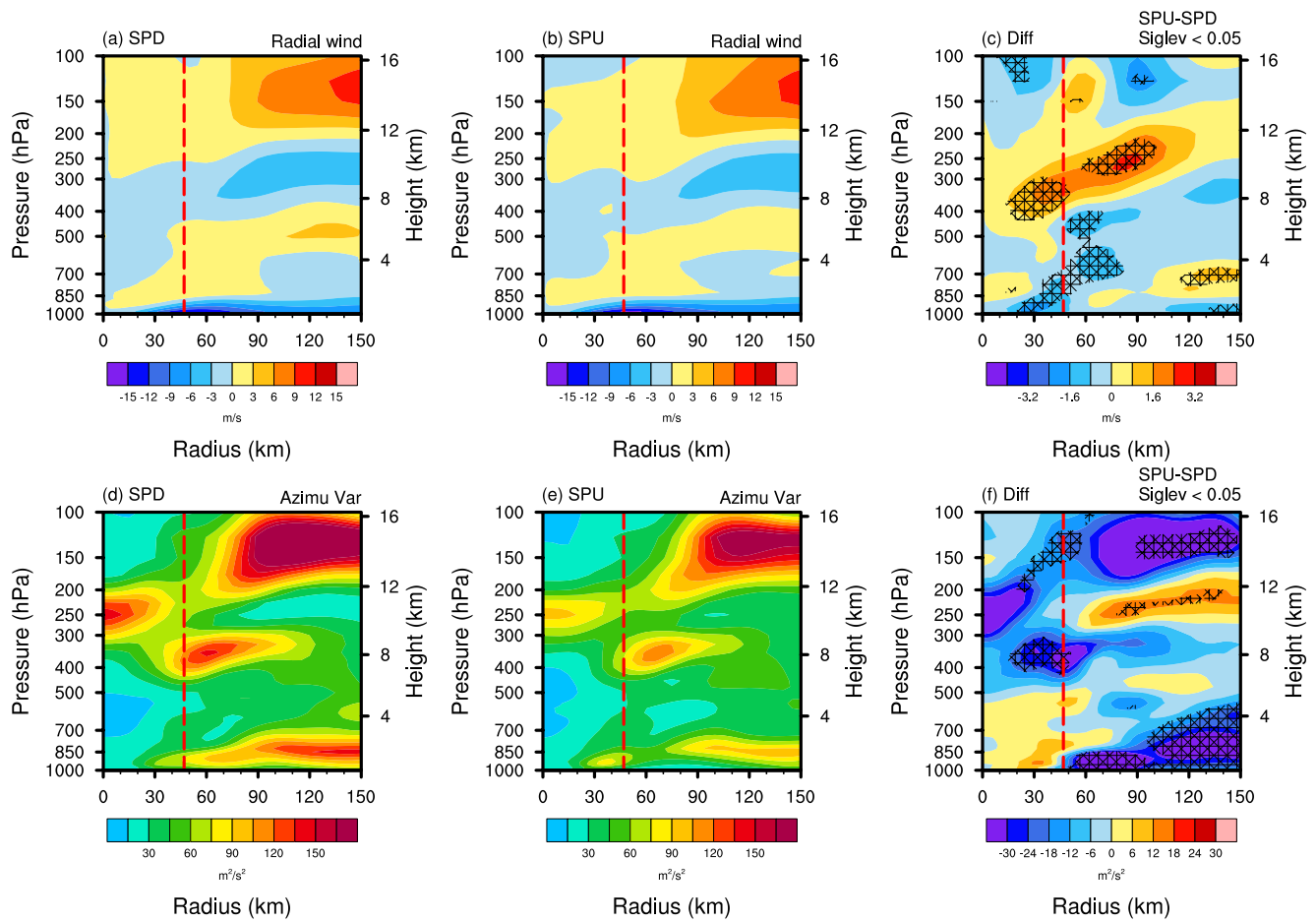
Figure 4. Radius–height plots of the ensemble-average azimuthal mean radial wind speed (unit: m/s) and the variance of the radial wind (unit: m²/s²) for the (a), (d) SPD and (b), (e) SPU members. (c), (f) Differences in the radial wind speed (unit: m/s) and the variance of the radial wind speed between the SPD and SPU members (SPU − SPD). The red dashed line is the average RMW at the height of 10 m. The gridded regions indicate statistical significance at the 95% confidence level.

decomposition to extract the different azimuthal wavenumber components of the initial wind field for each vertical level. Figure 5 shows the wavenumber analysis of the surface wind speed for the SPD and SPU members. Judt et al. (2016) showed that the 0, 1 and 2–5 wavenumber components represent the mean vortex, the vortex-scale asymmetry, and the storm rainbands, respectively, whereas the higher-order wave numbers are related to smaller mesoscale and convective-scale processes. The low wavenumber structures (wavenumbers 0–5) for the SPD and SPU members (Figures 5a and 5b) were consistent with those of the full field of the surface wind speed shown in Figures 2a and 2b, respectively. We also found that the low wavenumber structure of the surface wind in the west of the storm was significantly weaker for the SPD members than for the SPU members (Figure 5c).

There was little difference in the distribution of higher wave numbers, and both the SPD and SPU members showed an asymmetry with the maximum/minimum amplitudes in the southwest (Figures 5d and 5e). The ensemble-average azimuthal phase and amplitude of the higher wavenumber structure at a radius of about 150 km from the storm center was different for the SPD and SPU members, although the differences were not statistically significant at the 95% confidence level (Figure 5f).

For the surface wind speed, the azimuthal variance of the wavenumber 1 and 2 components showed two peaks for the SPD members, with a slower rate of decay inside the RMW, whereas there was a peak closer to the center of the storm and a significant decrease in the azimuthal variance for the SPU members inside the RMW (Figures 5g and 5h). The peak variance for the SPD members was much smaller than for the SPU members. In addition to the lowest wavenumber components, the azimuthal variance of wavenumbers 3–5 was slightly different between the SPD and SPU members. The difference between the structure of the two low wave numbers in the surface wind speed was the clearest distinction between the SPD and SPU members.
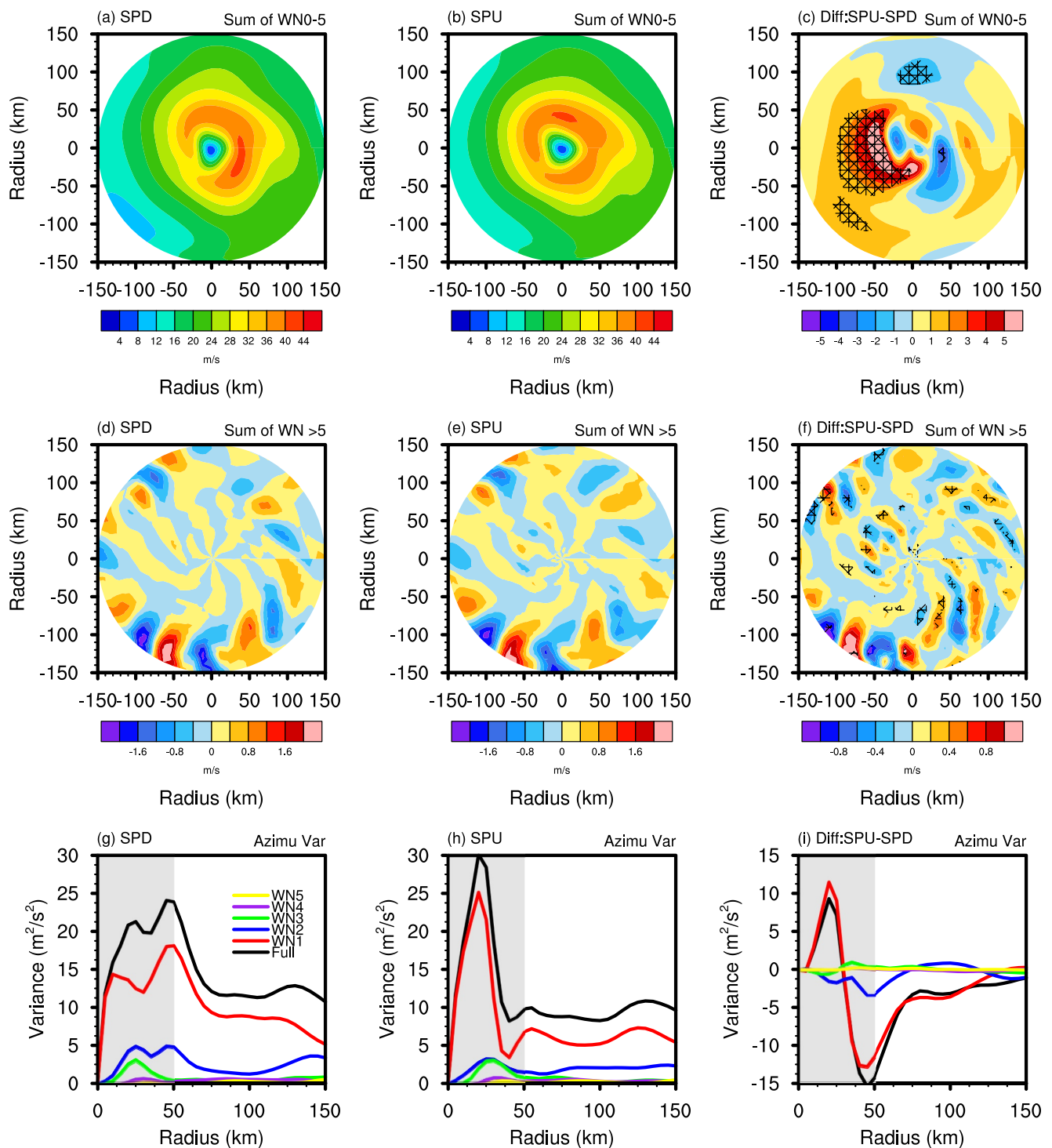
Figure 5. Sum of the wavenumber 0–5 and wavenumber >5 components of the azimuthal surface wind field at the initial time for the (a), (d) SPD and (b), (e) SPU members. The mean azimuthal-average variance of the original surface wind field (black, as depicted by the full field) for the SPD and SPU members and the mean azimuthal-average variance for wavenumber 1 (red), 2 (blue), 3 (green), 4 (purple) and 5 (yellow). (c), (f) Differences between the SPD and SPU members (Diff = SPU − SPD) for the wavenumber 0–5 and wavenumber >5 components of the mean azimuthal surface wind field and (g) the mean azimuthal average variance of each wavenumber component. Gray shaded regions represent the distance from the center to 50 km. The gridded regions indicate statistical significance at the 95% confidence level.
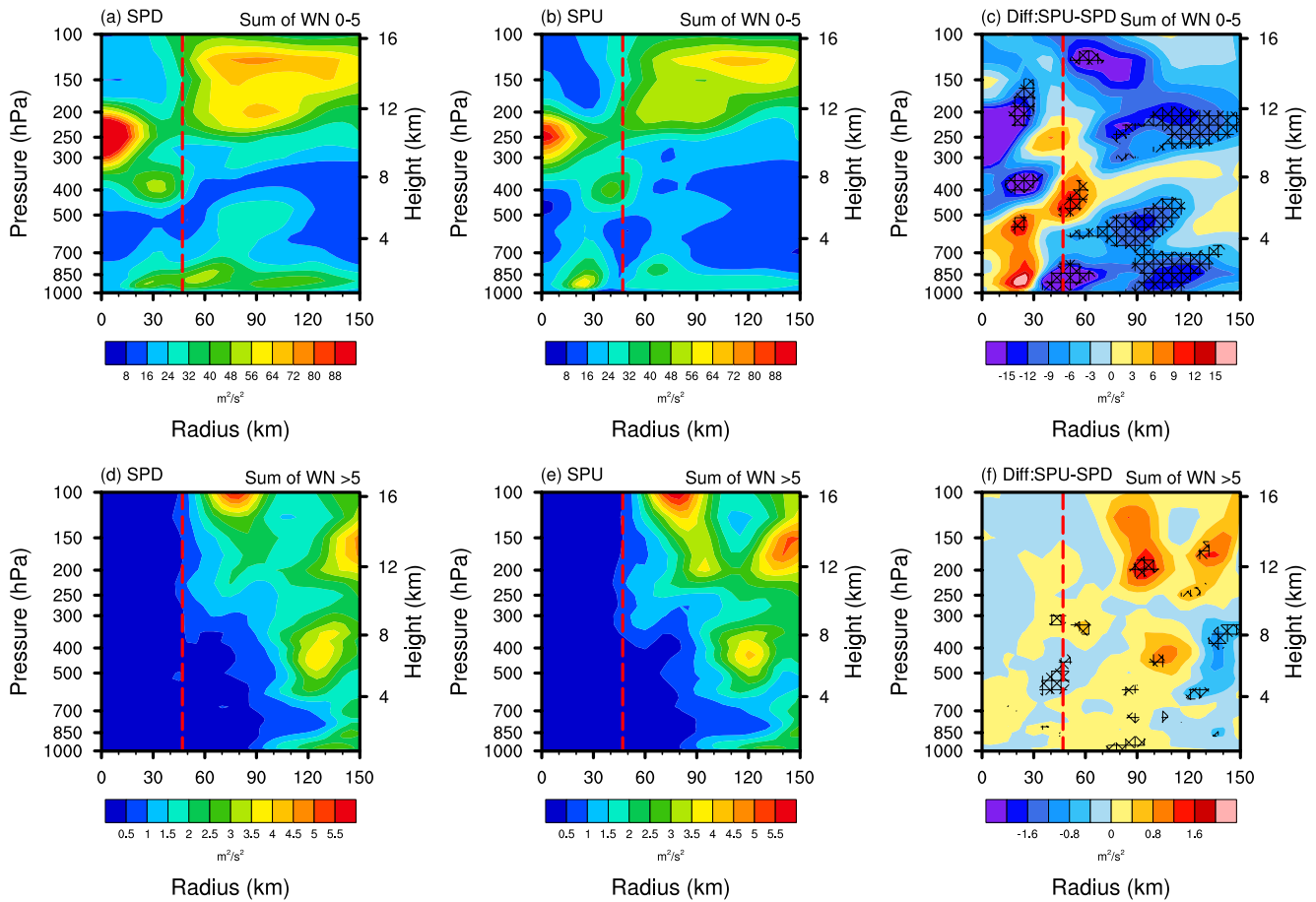
Figure 6. Averaged azimuthal variance of the wavenumber 0–5 and wavenumber >5 components of the initial tangential wind as a function of the radius to the center and altitude (isobaric level and height) for the (a), (d) SPD and (b), (e) SPU members. (c), (f) Differences between the SPD and SPU members. The red dashed line is the average RMW at the height of 10 m. The gridded regions indicate statistical significance at the 95% confidence level.

Figures 6a–6c shows the ensemble-average azimuthal variance of the wavenumber 0–5 components for the tangential wind, which was roughly consistent with the vertical structure of the total variance of the original tangential wind shown in Figures 3e and 3f. The sum of the higher wavenumber components (wavenumbers >5) for both the SPD and SPU members shows the ensemble-average azimuthal variance minimized inside the RMW and that there were two maximized variance centers outside the 60-km radius of the storm above the height of 12 km. There was a significant increase in the azimuthal variance with increasing radial distance (Figures 6d and 6e). A key difference between the SPD and SPU members in the azimuthal variance of the higher wavenumber components was detected for the 90-km radius at the height of 12 km. Another small difference was located 35 km from the storm at a height of approximately 4 km (Figure 6f).

The azimuthal variance structures of the low wavenumber components of the radial wind compared well with those of the original radial wind (Figures 4a and 4b). The ensemble average of the SPU members showed a significantly stronger variance outside the RMW at upper and lower levels (Figure 7c), similar to those shown in Figure 4f (significant at the 95% confidence level). A minimum of the azimuthal variance of the high wavenumber radial wind was seen within 30 km of the center of the storm (Figures 7d and 7e), and there was no statistically significant difference between the two sets of ensemble members. The azimuthal variance in the outer core was greater for the SPD members than for the SPD members, but the difference was only slightly significant at the upper level (Figure 7f).

In summary, the two sets of ensemble members showed very different distributions at the lower wave numbers for both the tangential and radial winds, but no systematic significant difference for the higher wave numbers. These results indicate that the lower-order asymmetrical wave numbers made a more important contribution to the intensification of the storm than the higher-order wave numbers.
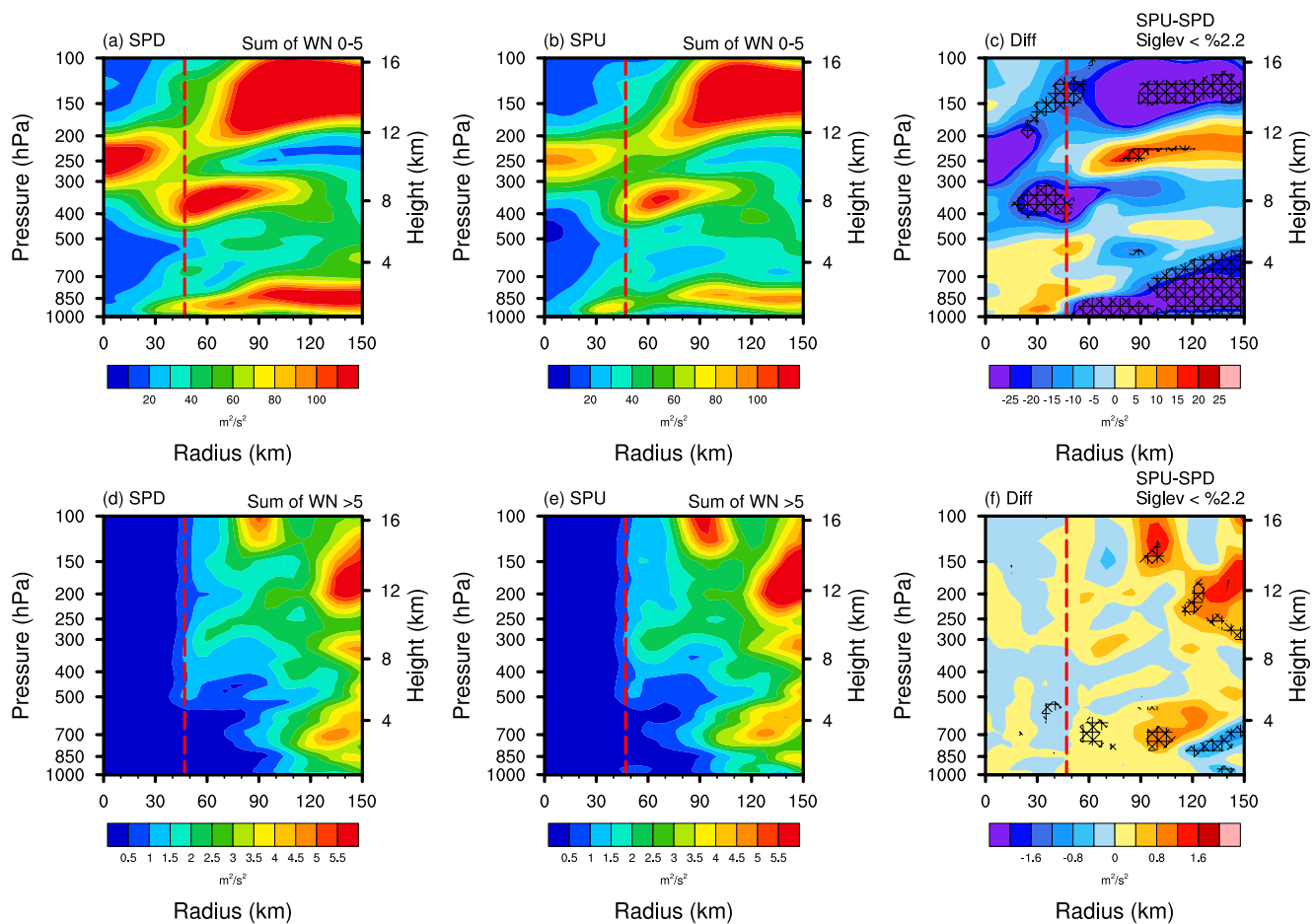
Figure 7. Averaged azimuthal variance of the wavenumber 0–5 and wavenumber >5 components of the initial radial wind as a function of the radius to the center and altitude (isobaric level and height) for the (a), (d) SPD and (b), (e) SPU members. (c), (f) Differences between the SPD and SPU members. The red dashed line is the average RMW at the height of 10 m. The gridded regions indicate statistical significance at the 95% confidence level.

3.3. Hypothesis Testing With Model Simulation

Through ensemble clustering analysis, Section 3.2 led to the hypothesis that the key differences between the SPU and SPD ensemble members were the structure and magnitude of the low wavenumber components. To further verify this hypothesis, we initialized five sets of retrospective HWRF ensemble forecasts by only retaining the low-order wavenumber components of the wind speed frequency spectra (e.g., wavenumbers 0–1, 0–2, 0–3, 0–4, and 0–5). The model configuration, model physics, and boundary conditions remained the same as described in Subsection 2.1.

The forecasts of the MSLP and MWS initialized from the full field (as depicted by the sum of all the wave numbers or the original field) and their low wavenumber components were verified against the best-track estimates (Figure 8). We used Ens 09 and Ens 17 to represent the SPD and SPU members, respectively, because they had the smallest and largest rates of change in intensity (Table 1). Over the 24-hr period, there was no difference in the forecasts of peak intensity between the SPD and SPU members, with a peak value of the MWS of approximately 80 m/s (Figures 8c and 8d). However, in contrast with the SPU members, there was a persistent MWS SPD during the first 6 hr for the SPD members for all sets of experiments retaining different low wave numbers. The experiment retaining only wavenumbers 0–1 had the slowest rate in returning to SPU following SPD, reaching a weakest peak intensity.

For the SPU members, although the initial analyses of the wind speed retained only the lower wavenumber components, the evolution of intensity was similar for all members and was not significantly different from the experiment in which the initial analysis used the full wind field. The change in intensity for the SPU members
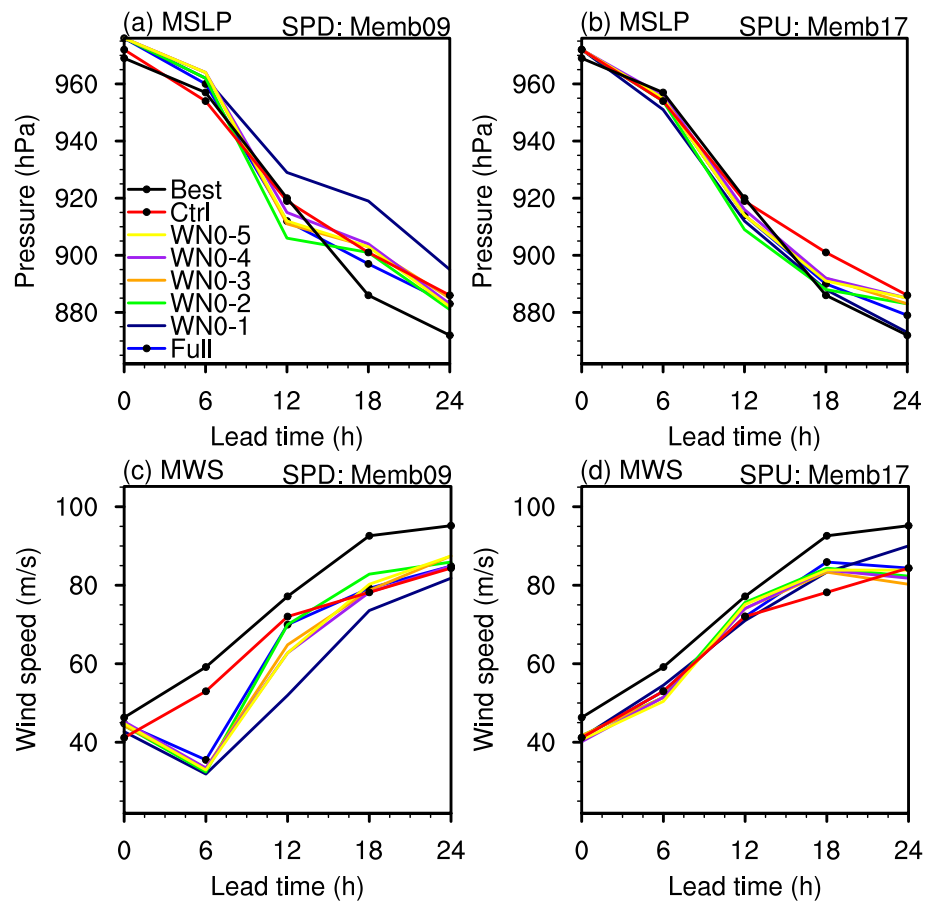
Figure 8. Forecasts of the MSLP (unit: hPa) and MWS (unit: m/s) as a function of lead time for the (a), (c) SPD and (b), (d) SPU members initialized with the full field (blue) and initialized with lower-order wavenumber components of the wind speed field within 150 km of the center of the storm: wavenumbers 0–1 (navy blue), 0–2 (green), 0–3 (orange), 0–4 (purple), and 0–5 (yellow). The red and black lines represent the control (Ctrl) and best-track (Best) forecasts.

was more consistent with the best track in the entire first 12 hr than for the SPD members (Figure 8d). Meanwhile, we further examined the spread of MSLP and MWS for all sets of experiments retaining a full field and different low wavenumber components in the SPD and SPU members. It was found that there was no significant difference in the spread of the MSLP and MSW between the SPD and SPU members at the first 6 hr, but the uncertainty (spread) of both MSLP and MSW in the SPD members was significantly larger than that in the SPU members after the first few hours (not shown).

Moreover, to further verify the hypothesis that the differences in the low-wavenumber asymmetries can induce SPD issue, we initialized additional HWRF forecasts by solely exchanging the low wavenumber (wavenumber 0–5) components of the wind speed field between SPD and SPU members (Figure 9). Similarly, Ens 09 and Ens 17 were used to represent the SPD and SPU members, respectively. The model configuration, model physics, thermal variables fields in the initial condition, and boundary conditions remained the same as described in Subsection 2.1. As can be seen from Figure 9c, when the SPD member was initialized with the wavenumber 0–5 wind components from the SPU member, the SPD issue was found to be significantly alleviated and the corresponding intensity forecast was improved (M09-M09WN05 vs. M09-M17WN05). Vice versa, when the SPU member was initialized with the wavenumber 0–5 wind components from the SPD member, a slightly SPD issue would occur and lead to the substantially significant degradation of the short-term intensity forecast (Figure 9d, M17-M09WN05 vs. M17-M17WN05). It is well known that the of the low wavenumber components of the initial wind speed include both the axisymmetric and asymmetric structures. Therefore, the results presented in this section, together with those in Section 3.2, suggest that both the axisymmetric and asymmetric structures of the low wavenumber components for the initial wind speed may have played an important role in the prediction of the change in storm intensity, especially during the intensification phase in the first 6 hr.
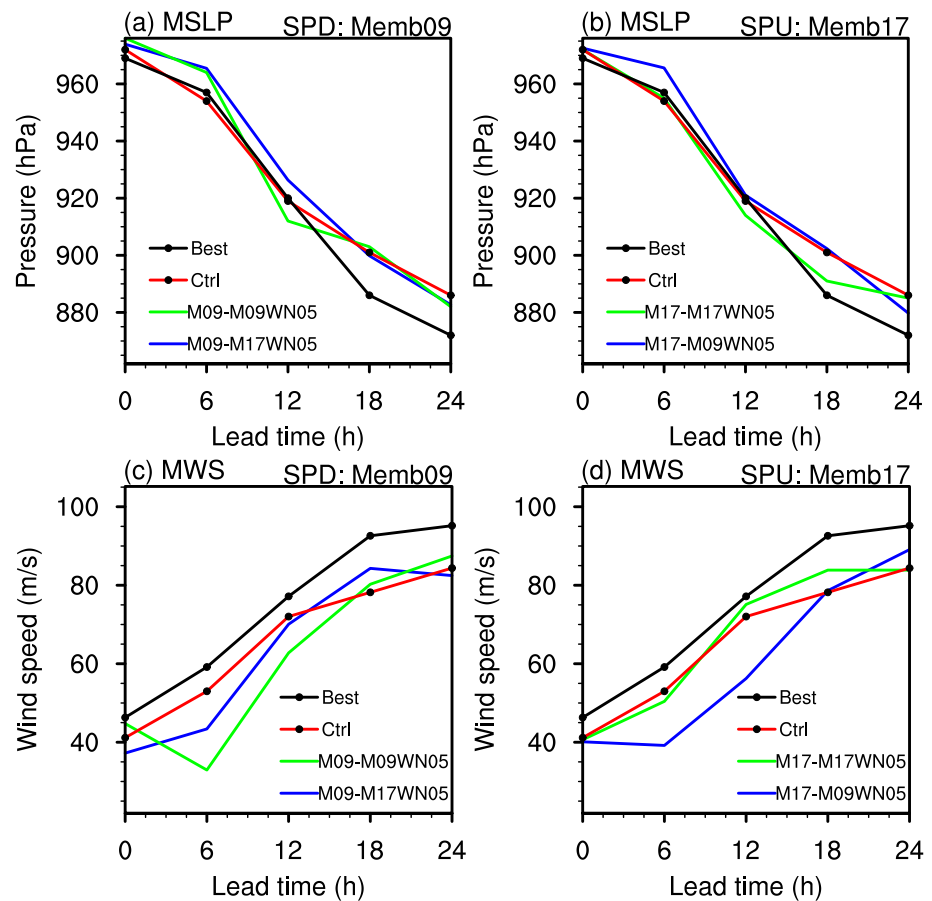
Figure 9. Forecasts of the MSLP (unit: hPa) and MWS (unit: m/s) as a function of lead time for the numerical experiments initialized with the original wavenumber 0–5 components of the wind speed field (blue) and initialized with the replaced wavenumber 0–5 components of the wind speed field. Ens 09 (a), (c) and 17 (b), (d) represent the SPD and SPU members, respectively. The M09-M09WN05 and M17-M17WN05 (green lines) indicate that Ens 09 and 17 were initialized with their own wavenumber 0–5 components of the wind field, respectively, while the M09-M17WN05 and M17-M09WN05 (blue lines) indicated that Ens 09 and 17 were initialized with the wavenumber 0–5 components of the initial wind field from each other. The red and black lines represent the control (Ctrl) and best-track (Best) forecasts.

4. Summary and Discussion

We examined the inner-core structure of the initial wind field between the SPD and SPU members in predictions of the intensification of Hurricane Patricia (2015) through ensemble clustering analysis. Figure 10 is a schematic diagram summarizing the key differences between these two sets of members (SPU−SPD). The surface wind speeds in the west of the storm were stronger for the SPU members than for the SPD members. The SPU members showed more significant azimuthal asymmetry in the surface winds than the SPD members. The maximum asymmetry for the SPU members occurred inside the RMW of the storm, whereas the maximum asymmetry for the SPD members was apparent at the RMW (Figure 2). In terms of the primary circulation, there was a stronger decay of the tangential winds between the heights of 4 and 12 km in the SPD members than the SPU members. The tangential winds outside the RMW of the storm were therefore much stronger for the SPU members than for the SPD members (Figure 10a). The vertical decay of the tangential winds in the interior flow was indicative of the vortex SPD, consistent with previous theoretical and observational studies (Montgomery et al., 2001; Rogers et al., 2013). The variance of the tangential wind for the SPU members inside the RMW below 8 km was larger than that for the SPD members, while the former was smaller than the latter outside the RMW (Figure 10b). Additionally, the SPU members showed a stronger inflow near the surface and strong outflow between the heights of 8 and 12 km than the SPD members, which contributed to the intensification during the first 6 hr. The magnitude of the peak azimuthal variance of radial wind for the SPD members was greater than that of the SPU members at both lower and upper levels.
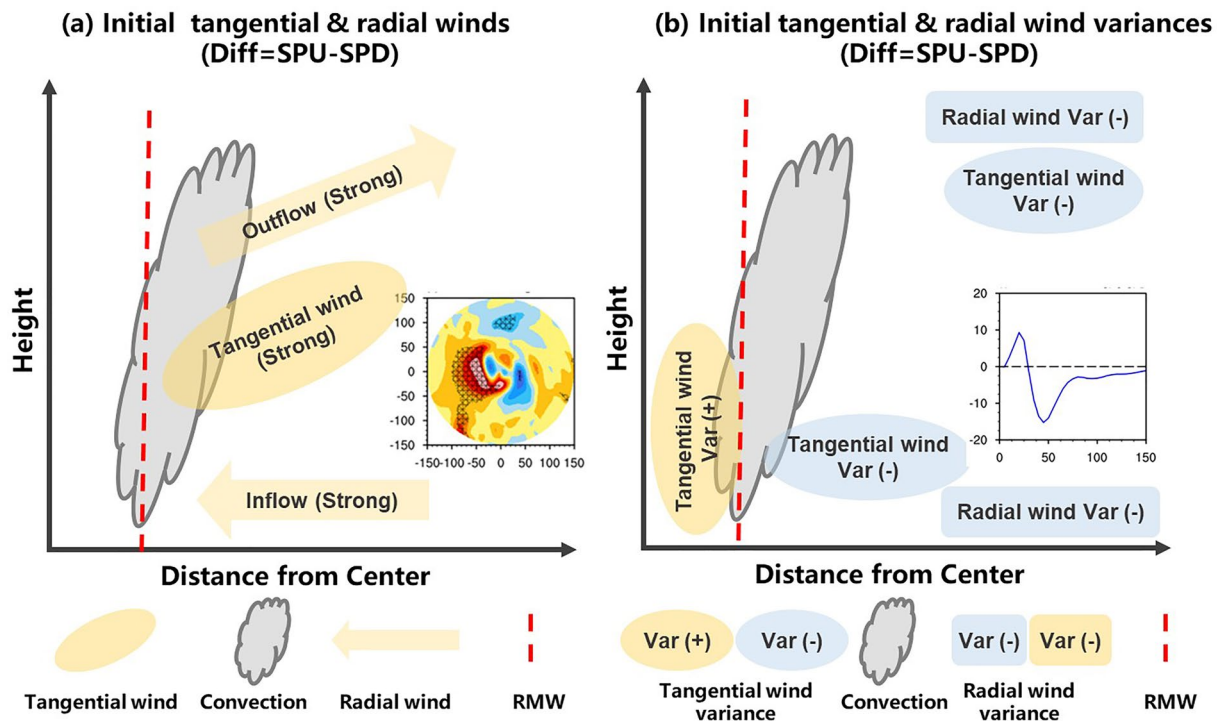
Figure 10. Schematic diagram summarizing the key differences in the (a) tangential and radial winds and (b) their variances in the inner-core structure between the SPD and SPU members.

Wavenumber analysis suggested that the magnitude and asymmetry of the full wind field were dominated by the lower wavenumber components of the wind field for both the SPD and SPU members. There were statistically significant differences in the lower wavenumber components (wavenumbers 0–5) of the tangential and radial winds between the SPD and SPU members, but only slight differences in the higher wavenumber components (wavenumbers >5). As pointed out by Judt et al. (2016), the low wavenumber components represent the mean vortex, the vortex-scale asymmetry, and the storm rainbands, respectively, whereas the higher-order wave numbers are related to smaller mesoscale and convective-scale processes. The SPD issue in some ensemble members can therefore be attributed to the suboptimum initial analyses of the tangential and radial winds, including their vortex-scale asymmetries, especially for the low wavenumber components, in the initial conditions. These results therefore infer a need for further data assimilation and targeted observation research. Given that an accurate representation of the structure of the inner core in the initial conditions is essential in forecasts of TC intensity, one of the critical pathways to improving TC intensity forecasts is the development and implementation of advanced techniques for the assimilation of conventional, radar and satellite observations inside the inner core.

Moreover, previous studies suggest that the SPD issue at early lead times can be damaging to intensity predictions in the HWRF model, with a significantly negative intensity bias for strong TCs (Tallapragada et al., 2014; Tong et al., 2018). However, Hurricane Patricia weakened rapidly and eventually made landfall after 24 hr, and the differences between the SPD and SPU members were therefore minimized due to the interaction with land. The difference in the storm intensity bias was limited to within the 18 hr-forecast only.

On a final note, whilst this study has revealed some interesting findings by exploring the consequences of independent effects of the low wavenumber structure in the initial vortex wind analyses on the prediction of the intensification of Hurricane Patricia (2015), the intensity change of a TC is generally associated with multiple factors, such as boundary-layer moisture, vertical-vortex structure, and warm-core structure. To further alleviate the SPD problem and improve storm intensity forecasts, additional research using high-resolution ensemble forecasts into the cause-and-effect role in hurricane intensification is a worthy avenue of investigation in future work.

Data Availability Statement

The best-track estimates for Hurricane Patricia (2015) are available at https://www.nhc.noaa.gov/?epac. The boundary conditions for the outermost domain in the ensemble experiments can be download from https://www.ncei.noaa.gov/products/weather-climate-models/global-forecast.

References

Brown, B. R., & Hakim, G. J. (2015). Sensitivity of intensifying Atlantic hurricanes to vortex structure. *Quarterly Journal of the Royal Meteorological Society*, *141*(692), 2538–2551. https://doi.org/10.1002/qj.2540

Callaghan, J. (2017). Asymmetric inner core convection leading to tropical cyclone intensification. *Tropical Cyclone Research and Review*, *8*(2), 95–102. https://doi.org/10.1016/j.tcrr.2019.07.009

Cangialosi, J. P., Blake, E., DeMaria, M., Penny, A., Latto, A., Rappaport, E., & Tallapragada, V. (2020). Recent progress in tropical cyclone intensity forecasting at the National Hurricane Center. *Weather and Forecasting*, *35*(5), 1913–1922. https://doi.org/10.1175/waf-d-20-0059.1

Chen, H., & Gopalakrishnan, S. G. (2015). A study on the asymmetric rapid intensification of Hurricane Earl (2010) using the HWRF system. *Journal of the Atmospheric Sciences*, *72*(2), 531–550. https://doi.org/10.1175/Jas-D-14-0097.1

Chen, X. M., Zhang, J. A., & Marks, F. D. (2019). A thermodynamic pathway leading to rapid intensification of tropical cyclones in shear. *Geophysical Research Letters*, *46*(15), 9241–9251. https://doi.org/10.1029/2019gl083667

DeMaria, M., Sampson, C. R., Knaff, J. A., & Musgrave, K. D. (2014). Is tropical cyclone intensity guidance improving? *Bulletin of the American Meteorological Society*, *95*(3), 387–398. https://doi.org/10.1175/bams-d-12-00240.1

Emanuel, K., & Zhang, F. Q. (2016). On the predictability and error sources of tropical cyclone intensity forecasts. *Journal of the Atmospheric Sciences*, *73*(9), 3739–3747. https://doi.org/10.1175/Jas-D-16-0100.1

Feng, J., & Wang, X. (2019). Impact of assimilating upper-level dropsonde observations collected during the TCI field campaign on the prediction of intensity and structure of Hurricane Patricia (2015). *Monthly Weather Review*, *147*(8), 3069–3089. https://doi.org/10.1175/mwr-d-18-0305.1

Feng, J., & Wang, X. (2021). Impact of increasing horizontal and vertical resolution during the HWRF hybrid EnVar data assimilation on the analysis and prediction of Hurricane Patricia (2015). *Monthly Weather Review*, *149*(2), 419–441. https://doi.org/10.1175/mwr-d-20-0144.1

Han, J., & Pan, H.-L. (2006). Sensitivity of hurricane intensity forecast to convective momentum transport parameterization. *Monthly Weather Review*, *134*(2), 664–674. https://doi.org/10.1175/mwr3090.1

Hong, S.-Y., & Pan, H.-L. (1996). Nonlocal boundary layer vertical diffusion in a medium-range forecast model. *Monthly Weather Review*, *124*(10), 2322–2339. https://doi.org/10.1175/1520-0493(1996)124<2322:nblvdi>2.0.co;2

Jones, S. C. (1995). The evolution of vortices in vertical shear. I: Initially barotropic vortices. *Quarterly Journal of the Royal Meteorological Society*, *121*(524), 821–851. https://doi.org/10.1002/qj.49712152406

Judt, F., Chen, S. S., & Berner, J. (2016). Predictability of tropical cyclone intensity: Scale-dependent forecast error growth in high-resolution stochastic kinetic-energy backscatter ensembles. *Quarterly Journal of the Royal Meteorological Society*, *142*(694), 43–57. https://doi.org/10.1002/qj.2626

Kaplan, J., & DeMaria, M. (2003). Large-scale characteristics of rapidly intensifying tropical cyclones in the North Atlantic basin. *Weather and Forecasting*, *18*(6), 1093–1108. https://doi.org/10.1175/1520-0434(2003)018<1093:lcorit>2.0.co;2

Kwon, Y. C., Lord, S., Lapenta, B., Tallapragada, V., Liu, Q., & Zhang, Z. (2010). Sensitivity of air-sea exchange coefficients (Cd and Ch) on hurricane intensity. *Preprints, 29th Conference on Hurricanes and Tropical Meteorology*.

Lacis, A. A., & Hansen, J. (1974). A parameterization for the absorption of solar radiation in the earth's atmosphere. *Journal of the Atmospheric Sciences*, *31*(1), 118–133. https://doi.org/10.1175/1520-0469(1974)031<0118:apftao>2.0.co;2

Lang, S., Leutbecher, M., & Jones, S. (2012). Impact of perturbation methods in the ECMWF ensemble prediction system on tropical cyclone forecasts. *Quarterly Journal of the Royal Meteorological Society*, *138*(669), 2030–2046. https://doi.org/10.1002/qj.1942

Leutbecher, M., & Palmer, T. N. (2008). Ensemble forecasting. *Journal of Computational Physics*, *227*(7), 3515–3539. https://doi.org/10.1016/j.jcp.2007.02.014

Lu, X., & Wang, X. (2019). Improving hurricane analyses and predictions with TCI, IFEX field campaign observations, and CIMSS AMVs using the advanced hybrid data assimilation system for HWRF. Part I: What is missing to capture the rapid intensification of Hurricane Patricia (2015) when HWRF is already initialized with a more realistic analysis? *Monthly Weather Review*, *147*(4), 1351–1373. https://doi.org/10.1175/mwr-d-18-0202.1

Montgomery, M. T., Kilroy, G., Smith, R. K., & Črnivec, N. (2020). Contribution of mean and eddy momentum processes to tropical cyclone intensification. *Quarterly Journal of the Royal Meteorological Society*, *146*(732), 3101–3117. https://doi.org/10.1002/qj.3837

Montgomery, M. T., & Smith, R. K. (2018). Comments on "Revisiting the balanced and unbalanced aspects of tropical cyclone intensification"[J]. *Journal of the Atmospheric Sciences*, *75*(7), 2491–2496. https://doi.org/10.1175/jas-d-17-0323.1

Montgomery, M. T., Snell, H. D., & Yang, Z. (2001). Axisymmetric spindown dynamics of hurricane-like vortices. *Journal of the Atmospheric Sciences*, *58*(5), 421–435. https://doi.org/10.1175/1520-0469(2001)058<0421:asdohl>2.0.co;2

Nystrom, R. G., & Zhang, F. Q. (2019). Practical uncertainties in the limited predictability of the record-breaking intensification of Hurricane Patricia (2015). *Monthly Weather Review*, *147*(10), 3535–3556. https://doi.org/10.1175/mwr-d-18-0450.1

Persing, J., Montgomery, M. T., McWilliams, J. C., & Smith, R. K. (2013). Asymmetric and axisymmetric dynamics of tropical cyclones. *Atmospheric Chemistry and Physics*, *13*(24), 12299–12341. https://doi.org/10.5194/acp-13-12299-2013

Qin, N. N., & Zhang, D. L. (2018). On the extraordinary intensification of Hurricane Patricia (2015). Part I: Numerical experiments. *Weather and Forecasting*, *33*(5), 1205–1224. https://doi.org/10.1175/Waf-D-18-0045.1

Reasor, P. D., Eastin, M. D., & Gamache, J. F. (2009). Rapidly intensifying hurricane Guillermo (1997). Part I: Low-Wavenumber structure and evolution. *Monthly Weather Review*, *137*(2), 603–631. https://doi.org/10.1175/2008mwr2487.1

Reasor, P. D., Montgomery, M. T., Marks, F. D., & Gamache, J. F. (2000). Low-wavenumber structure and evolution of the hurricane inner core observed by airborne dual-Doppler radar. *Monthly Weather Review*, *128*(6), 1653–1680. https://doi.org/10.1175/1520-0493(2000)128<1653:lwsaeo>2.0.co;2

Rogers, R., Reasor, P., & Lorsolo, S. (2013). Airborne Doppler observations of the inner-core structural differences between intensifying and steady-state tropical cyclones. *Monthly Weather Review*, *141*(9), 2970–2991. https://doi.org/10.1175/mwr-d-12-00357.1

Rogers, R. F., Aberson, S., Bell, M. M., Cecil, D. J., Doyle, J. D., Kimberlain, T. B., et al. (2017). Rewriting the tropical cyclone record books the extraordinary intensification of Hurricane Patricia (2015). *Bulletin of the American Meteorological Society*, *98*(10), 2091–2112. https://doi.org/10.1175/Bams-D-16-0039.1

Schoenberg Ferrier, B. (1994). A double-moment multiple-phase four-class bulk ice scheme. Part I: Description. *Journal of the Atmospheric Sciences*, *51*, 249–280. https://doi.org/10.1175/1520-0469(1994)051<0249:admmpf>2.0.co;2

Schwarzkopf, M. D., & Fels, S. B. (1991). The simplified exchange method revisited: An accurate, rapid method for computation of infrared cooling rates and fluxes. *Journal of Geophysical Research*, *96*(D5), 9075–9096. https://doi.org/10.1029/89jd01598

Smith, R. K., Montgomery, M. T., & Van Sang, N. (2009). Tropical cyclone spin-up revisited. *Quarterly Journal of the Royal Meteorological Society*, *135*(642), 1321–1335. https://doi.org/10.1002/qj.428

Tallapragada, V., Kieu, C., Kwon, Y., Trahan, S., Liu, O., Zhang, Z., & Kwon, L. H. (2014). *Hurricane weather research and forecasting (HWRF) model: 2014 scientific documentation* (p. 105). NCAR Development Testbed Center Report. Retrieved from http://www.dtcenter.org/HurrWRF/users/docs/scientific_documents/HWRFv3.6a_ScientificDoc.pdf

Tong, M., Sippel, J. A., Tallapragada, V., Liu, E., Kieu, C., Kwon, I.-H., et al. (2018). Impact of assimilating aircraft reconnaissance observations on tropical cyclone initialization and prediction using operational HWRF and GSI ensemble–variational hybrid data assimilation. *Monthly Weather Review*, *146*(12), 4155–4177. https://doi.org/10.1175/mwr-d-17-0380.1

Toth, Z., & Kalnay, E. (1997). Ensemble forecasting at NCEP and the breeding method. *Monthly Weather Review*, *125*(12), 3297–3319. https://doi.org/10.1175/1520-0493(1997)125<3297:efanat>2.0.co;2

Vukicevic, T., Uhlhorn, E., Reasor, P., & Klotz, B. (2014). A novel multi-scale intensity metric for evaluation of tropical cyclone intensity forecasts. *Journal of the Atmospheric Sciences*, *71*(4), 1292–1304. https://doi.org/10.1175/jas-d-13-0153.1

Wang, C., Zeng, Z., & Ying, M. (2020). Uncertainty in tropical cyclone intensity predictions due to uncertainty in initial conditions. *Advances in Atmospheric Sciences*, *37*(3), 278–290. https://doi.org/10.1007/s00376-019-9126-6

Wang, Y., & Holland, G. J. (1996). Tropical cyclone motion and evolution in vertical shear. *Journal of the Atmospheric Sciences*, *53*(22), 3313–3332. https://doi.org/10.1175/1520-0469(1996)053<3313:tcmaei>2.0.co;2

Zhou, C., Shao, H., & Bernardet, L. (2015). *Applications of the GSI-hybrid data assimilation for high-resolution tropical storm forecasts: Tackling the intensity spin-down issue in 2014 HWRF*. Preprints, 16th WRF Users Workshop.